Octreotide Scintigraphy for the Detection of Paragangliomas

Dik J. Kwekkeboom, Hero van Urk, Bernard K.H. Pauw, Steven W.J. Lamberts, Peter P.M. Kooij, Roel P.L.M. Hoogma and Eric P. Krenning

Departments of Nuclear Medicine, Medicine, Surgery and Otolaryngology, University Hospital Dijkzigt, Rotterdam, The Netherlands

Paragangliomas have neuroendocrine characteristics. We previously described successful in vivo visualization of various tumors of neuroendocrine origin after injection of the radiolabeled somatostatin analogue octreotide. In this study, we report the results of ^{111}In-octreotide scintigraphy in 34 patients referred because of known paragangliomas or in whom a paraganglioma was suspected and compared the results of octreotide scintigraphy with the outcomes of other imaging techniques used in the diagnosis or follow-up of these patients. Fifty of 53 (94%) known localizations in 25 patients with paragangliomas were visualized. In two patients, three localizations were missed during octreotide scintigraphy. Unexpected additional paraganglioma sites, not detected or not investigated with conventional imaging techniques, were found in 9 of 25 patients (36%) with known paragangliomas. In four of them, the supposed tumor localizations were thereafter also demonstrated with other imaging modalities. In eight of nine patients who were referred because of symptoms consistent with paraganglioma or follow-up after surgical removal of a paraganglioma, neither routine imaging nor octreotide scintigraphy revealed any abnormalities indicative of paraganglioma. We conclude that: (1) virtually all paragangliomas can be visualized using in vivo ^{111}In-octreotide scintigraphy and (2) because conventional imaging is usually limited to the site where a paraganglioma is clinically suspected, octreotide scintigraphy, because of the information it provides on potential tumor sites in the whole body, may be useful in detecting multicentricity or metastases in patients with paraganglioma.

J Nucl Med 1993; 34:873–878

Paragangliomas, or glomus tumors, are tumors of neural crest origin that arise from sympathetic or parasympathetic paraganglia. The most frequent paragangliomas are those of the head and neck, which are nonchromaffin and stem from parasympathetic paraganglia. Much rarer are paragangliomas of sympathetic origin, the majority of which are located in the thoraco-abdominal region. These tumors, like pheochromocytomas, arise from chromaffin tissue and frequently cause symptoms by overproduction of catecholamines (*1*).

About 9% of paragangliomas are familial (*2*). Multicentricity of paragangliomas is present in about 10% of unselected series, but may be as high as 32% in familial cases (*2,3*). Malignant behavior, characterized by spread in tissues not related to paraganglia, i.e., bone, soft tissue and viscera, occurs in about 10% of patients (*1,2,4*). Paragangliomas have neuroendocrine or amine precursor uptake and decarboxylation (APUD) characteristics. Immunostains for neuroendocrine markers such as neuron-specific enolase (NSE) are positive, and electron microscopy reveals secretory granules (*1*).

We previously described successful in vivo visualization of various tumors of neuroendocrine origin after the injection of a somatostatin analogue coupled to ^{123}I or ^{111}In (*5–9*). Also, successful in vivo visualization of 29 of 31 paragangliomas in 20 patients using an iodinated somatostatin analogue (^{123}I-Tyr^3-octreotide) was concisely reported (*7*). In this study, we report the results of ^{111}In-octreotide scintigraphy in another 34 consecutive patients referred because of known paragangliomas or in whom a paraganglioma was suspected and compared the results of octreotide scintigraphy with the outcomes of other imaging techniques used in the diagnosis or follow-up of these patients.

PATIENTS AND METHODS

Patients

Thirty-four patients who received ^{111}In-octreotide scintigraphy were studied (19 men, 15 women; mean age 47 yr, range 16–79 yr). Inclusion required either histologic or radiologic confirmation of a paraganglioma of a present or previously operated lesion or a history of paraganglioma-related signs and symptoms. In all patients, data on symptomatology, treatment and relevant conventional imaging had to be present. All patients gave informed consent to participate in the study, which was approved by the ethics committee of our hospital.

Methods

The biodistribution and metabolism of ^{111}In-[DTPA-D-Phe^1]-octreotide, as well as its capacity to visualize somatostatin recep-

Received Nov. 19, 1992; revision accepted Feb. 25, 1993.
For correspondence or reprints contact: D.J. Kwekkeboom, MD, University Hospital Dijkzigt, Room V 220, 40 Dr. Molewaterplein, 3015 GD Rotterdam, The Netherlands.

tor positive tumors in vivo, have been described previously (*10,11*).

The somatostatin analogue [DTPA-D-Phe^1]-octreotide (215–811) was obtained from Sandoz, Basel, Switzerland. [DTPA-D-Phe^1]-octreotide was coupled to ^{111}In as previously described (*12*). The labeling yield was higher than 97%. Indium-111-DTPA-D-Phe^1-octreotide (214–400 MBq) was injected in 34 patients. Planar images were obtained with a large field of view gamma camera (Counterbalance 3700 and ROTA II, Siemens Gammasonics, Erlangen, Germany), equipped with a medium-energy collimator. Static images were obtained 4 and 24 or 24 and 48 hr after injection of ^{111}In-octreotide. Preset counts for images obtained 4 and 24 hr after injection of ^{111}In-octreotide were 300,000 for the head and neck and 500,000 for the remainder of the body. The preset time for images obtained 48 hr after injection was 15 min (*11*). SPECT images obtained after 4 or 24 hr were available for 28 patients.

To define the tumors as visualized during this scanning procedure, we used a simple yes-or-no system. In each patient, the two subsequent scans (i.e., 4 and 24 hr or 24 and 48 hr after injection) were compared. As a rule, and especially in the abdomen, accumulation of radioactivity at an abnormal site was considered to represent somatostatin receptor binding only if it was present on the scintigrams of both standard imaging time points. The scintigrams from all 34 patients were reexamined by two of us together (DJK, EPK) without knowledge of the patient's identity, medical history or outcomes from other investigations. If the interpretations differed, they were discussed until an agreement was reached. Other conventional imaging was not structurally performed before or after octreotide scintigraphy.

The uptake of ^{111}In-octreotide in tumors was calculated in four patients. The background-corrected uptake in the tumor was measured and corrected for tissue absorption using CT scan images. Background radioactivity was measured in an area directly adjacent to the tumor.

RESULTS

Twenty-five patients were known to have paragangliomas and nine were referred because of symptoms consistent with paraganglioma or follow-up after surgical removal of a paraganglioma. A familial occurrence of paragangliomas was present in nine patients. Five of these patients were relatives. Eleven patients had surgery 4 mo to 23 yr previously. In eight of them, pathology proven paragangliomas had been removed. Two patients had received radiotherapy and one patient had also had chemotherapy.

In 25 patients, 53 paraganglioma localizations were visualized with conventional imaging techniques, including computed tomography (CT), ultrasound (US), angiography, MIBG scanning and bone scans. In two patients, an adrenal pheochromocytoma was also found (Table 1). With octreotide scintigraphy, 50 of 53 known paraganglioma sites and 1 of 2 known adrenal pheochromocytomas were visualized (Table 1). One of two carotid body paragangliomas in one patient, detected with US, as well as a bone metastasis suggested by bone scan and enlarged retroperitoneal lymph nodes demonstrated by CT scan in another patient, did not accumulate radioactivity during octreotide scintigraphy. SPECT studies, which were available for 28 patients, were in accordance with planar images in all instances. They were especially useful in patients with carotid body or vagal paragangliomas in order to differentiate between unilateral tumors which may visualize on both lateral planar images and true bilateral paragangliomas.

The initial findings with routine imaging techniques in Patients 1–6 were 10 carotid body paragangliomas and a pheochromocytoma. In five of these patients, all carotid body paragangliomas were clearly visualized on octreotide scintigraphy (Fig. 1). A recurrent carotid body paraganglioma measuring 7 mm in diameter was not visualized and one measuring 25 mm in diameter was visualized only faintly in Patient 6, who had bilateral surgery 12 yr previously. In Patient 4, in whom a bilateral carotid body paraganglioma had been found on US, subsequent octreotide scintigraphy suggested tumor localizations not only in the neck, but in the mediastinum as well (Fig. 2). Because of these findings, CT scanning of the neck was extended to include the thorax, in which two mediastinal lesions measuring 4 and 3 cm in diameter were detected.

In Patients 7–15, all 10 jugulotympanic paragangliomas were visualized during octreotide scintigraphy (Table 1, Fig. 3). In addition to the ten paragangliomas, two previously unrecognized carotid body paragangliomas, two vagal paragangliomas and one contralateral jugulotympanic paraganglioma were visualized during octreotide scintigraphy in three of nine patients (Table 1). In Patient 15, in whom preoperative CT scanning and US of the neck failed to demonstrate tumor localization other than a right-sided jugulotympanic paraganglioma, repeated CT scanning performed 7 mo after octreotide scintigraphy not only showed a recurrent tumor at the surgical site, but two additional lesions previously suggested during octreotide scintigraphy.

In Patients 16–25, multiple tumor sites were detected with conventional imaging techniques. In these 10 patients, 31 of 33 known paraganglioma sites accumulated ^{111}In-octreotide. In six patients, octreotide scintigraphy suggested tumor localizations at sites not recognized or not investigated with other techniques (Table 1; Patients 20–25). In Patient 21, a separate spot of radioactivity accumulation below the jugulotympanic paraganglioma was seen on planar images during octreotide scintigraphy. The SPECT images, however, suggested the lower hot spot to be connected with the upper (jugulotympanic) one, a finding which could be in agreement with local expanding growth of the jugulotympanic paraganglioma. Because there was no clinical suspicion of distant metastases in Patient 22, CT scanning and US were only performed on the skull and neck. The two paragangliomas known at that time were clearly visualized during octreotide scintigraphy. However, two additional sites of abnormal radioactivity accumulation, posterior in the lower thorax and between the kidneys, were also seen. Subsequent thin-slice CT scanning of the thorax and upper abdomen failed to reveal a lesion at the upper edge of the two sites seen during octreotide scintigraphy. However, a lesion with a

TABLE 1
Results of Conventional Imaging and Octreotide Scintigraphy in 34 Patients referred because of Paraganglioma

Patient no.	Conventional imaging	Presumed paraganglioma localizations	
		Conventional imaging	Octreotide scintigraphy
1	CT, US	CB (l)	CB (l)
2	US	CB (l)	CB (l)
3	US	CB (l + r)	CB (l + r)
4	CT, US	CB (l + r)	CB (l + r), two mediastinal spots
5	CT, US, MIBG	CB (l + r), Adrenal (pheo)	CB (l + r)
6	CT, US	CB (l + r)	Faint accumulation CB (r)
7	MRI, CT, US	JugTymp (l)	JugTymp (l)
8	MRI, CT, MIBG	JugTymp (l)	JugTymp (l)
9	CT, US, MIBG	JugTymp (l)	JugTymp (l)
10	CT	JugTymp (l + r)	JugTymp (l + r)
11	CT, US	JugTymp (r)	JugTymp (r)
12	CT, US, MRI	JugTymp (l)	JugTymp (l)
13	CT, US	JugTymp (l)	JugTymp (l), Vagal (l)
14	CT, Angio	JugTymp (l)	JugTymp (l), *CB* (l), JugTymp (r)
15	CT, US	JugTymp (r)	JugTymp (r), Vagal (r), CB (l)
16	CT, US	CB (l), JugTymp (r)	CB (l), JugTymp (r)
17	CT, US, Angio	CB (l + r), vagal (l), JugTymp (l)	CB (l + r), vagal (l), JugTymp (l)
18	CT, US	CB (l), vagal (l)	CB (l), vagal (l)
19	CT, US, Angio, MIBG	CB (l + r), vagal (l + r), JugTymp (r), adrenal (Pheo)	CB (l + r), vagal (l + r), JugTymp (r), adrenal
20	CT, US	CB (r), vagal (l), JugTymp (r)	CB (r), vagal (l), JugTymp (r), *CB (l)*
21	CT, US, Angio	CB (l), JugTymp (r)	CB (l), JugTymp (r), vagal (r)*
22	CT, US	CB (r), JugTymp (r)	CB (r), JugTymp (r), two dorsal median spots in lower thorax and between kidneys
23	CT, US, MIBG	Vagal (l), JugTymp (l)	Vagal (l), JugTymp (l), near thyroid, Parietal (r), two dorsal thoracal spots, one dorsal spot between kidneys, left thorax, three abdominal spots
24	CT, US, Bone scan	Vertebral metastasis (L3), Retroperitoneal lymph nodes BS: acromion *(r)*, 9th Rib, Th IX, L3	Spot medial to right kidney, two spots posterior median thorax, left pelvic region
25	CT	CB (l + r) extending to vagal (l + r), liver, metastases L1, retroperitoneal mass (l)	CB (l + r) extending to vagal (l + r), liver, two spots between kidneys, spot medial to left kidney, Posterior thorax
26	CT, US, Angio	None; aneurysm carotic artery (l + r)	None
27	CT, US, MRI	None; cholesteatoma	None
28	CT, US	None; chronic otitis	None
29	CT	None	None
30	CT, US, Angio	None	None
31	MIBG	None	None
32	MIBG	None	None
33	CT, US	None	None
34	CT	None	JugTymp (r)

*See text.
US = ultrasound; MIBG = ^{123}I-metaiodobenzylguanidine scintigraphy; Angio = angiography; Pheo = pheochromocytoma.

maximum diameter of 2.5 cm was found in the vertebral body. In Patient 23, who was referred because of hearing loss and tinnitus, a carotid body paraganglioma and a recurrent tumor in the scar tissue had been excised 23 and 22 yr previously, respectively. Conventional imaging demonstrated two paragangliomas in the head and neck region. With octreotide scintigraphy, nine additional spots throughout the body were seen, four of which corresponded with hot spots on a subsequent bone scan. In Patient 24, who had a metastasized paraganglioma without head or neck localization, all known localizations except a hot spot in the acromion noted during bone scanning and enlarged retroperitoneal lymph nodes found on CT were visualized during octreotide scintigraphy. An unexpected finding was accumulation of labeled octreotide in the left pelvic region, possibly representing a bone metastasis. In

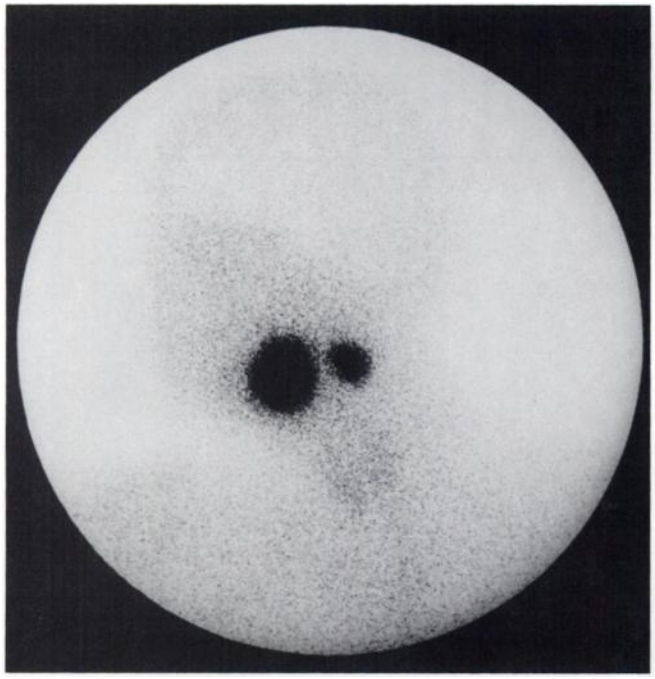

FIGURE 1. Left lateral image of the head and neck of Patient 3 24 hr after injection of ^{111}In-octreotide. Note the normal, faint accumulation of radioactivity in the thyroid and clear accumulation of radioactivity at the site of carotid body paragangliomas.

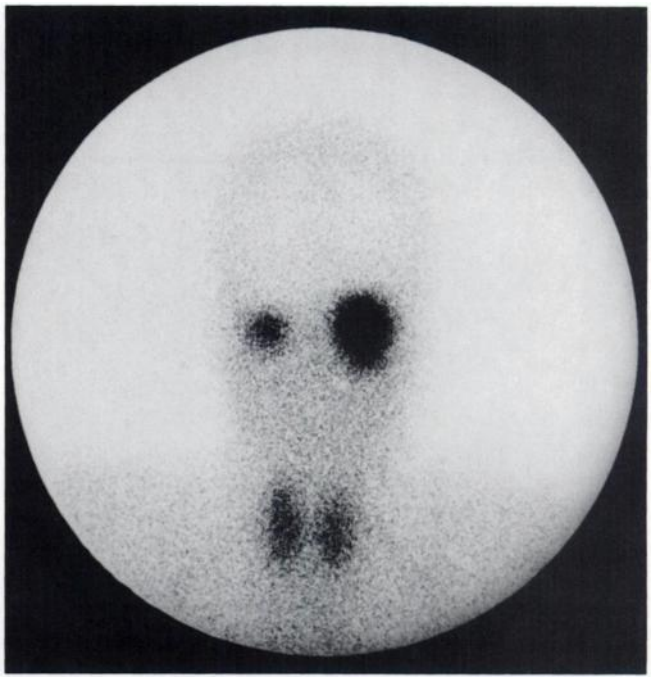

FIGURE 3. Anterior image of the head and neck of Patient 10 24 hr after injection of ^{111}In-octreotide. There is normal accumulation of radioactivity in the thyroid and accumulation of radioactivity at the site of bilateral jugulotympanic paragangliomas.

Patient 25, all known tumor sites were visualized during octreotide scintigraphy. An unexpected finding, not supported by conventional imaging, was a hot spot in the posterior thorax, implying a skeletal metastasis (Fig. 4).

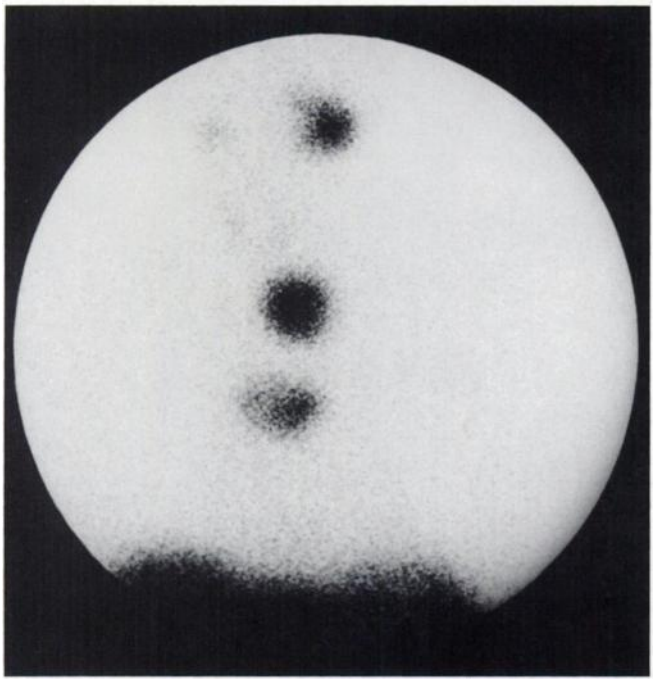

FIGURE 2. Anterior view of the neck and thorax of Patient 4 24 hr after injection of ^{111}In-octreotide. Note the normal uptake of radioactivity in the thyroid, liver and spleen (lower border). There is clear visualization of bilateral carotid body paragangliomas and two mediastinal tumors.

Patients 26–34 were referred because of symptoms consistent with paraganglioma (7 patients) or follow-up after surgical removal of a paraganglioma (2 patients). In eight of these patients, neither routine imaging nor octreotide scintigraphy revealed any abnormalities indicative of paraganglioma (Table 1). Only in Patient 34, who had surgery because of a carotid body paraganglioma 6 mo previously, abnormal accumulation of labeled octreotide was seen, suggesting a right-sided jugulotympanic paraganglioma. CT scanning at that time, however, was limited to the neck, so no confirmation of this finding was obtained.

Twenty-two unexpected additional paraganglioma sites not detected or investigated with conventional imaging techniques were found in 10 patients during octreotide scintigraphy. Five of these (in Patients 4, 15, and 22) were thereafter confirmed by CT scanning, whereas four localizations in one patient (Patient 23) corresponded with hot spots on a subsequent bone scan. Histologic confirmation of paraganglioma was obtained for one localization (Patient 4).

MIBG scanning was performed in seven patients (Table 1). In two of five patients with known paragangliomas, paraganglioma sites accumulated ^{123}I-MIBG (Patients 8 and 9, Table 1). In Patient 23, MIBG scanning resulted in only faint visualization of the skull metastasis and no accumulation of labeled MIBG in any of the other multiple paraganglioma localizations. In Patients 31 and 32, who had no otherwise proven paragangliomas, both MIBG and octreotide scintigraphy demonstrated no abnormalities.

The calculated uptake of ^{111}In-octreotide for four paraganglioma localizations in different patients are listed in

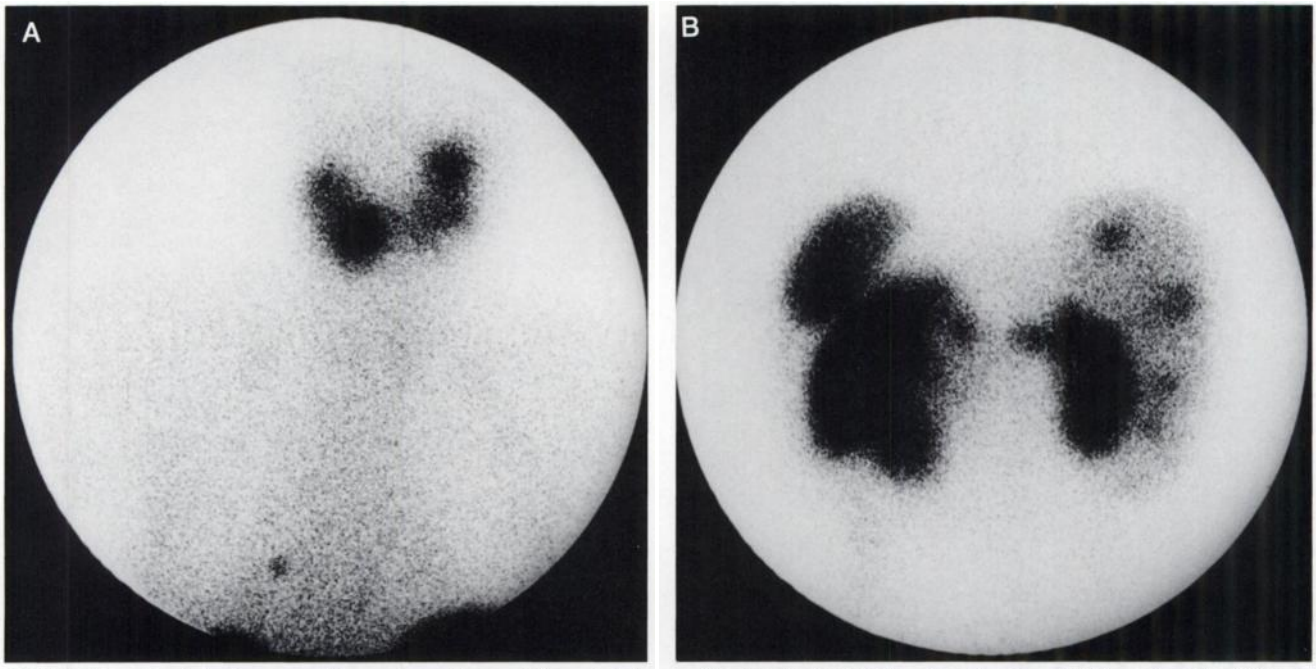

FIGURE 4. Posterior image of the neck and thorax (A) and abdomen (B) of Patient 25 24 hr after injection of ^{111}In-octreotide. (A) Note the abnormal bilateral uptake of radioactivity in the neck and a small area of increased radioactivity in the lower left thorax. (B) Normal uptake in the spleen, liver and kidneys. There is increased uptake in four areas in the liver, as well as medial to the upper edge of the right and left kidney, and below and medial to the left kidney.

Table 2. The tumor-to-background radioactivity ratio varied from 1.8 to 4.4. Radioactivity uptake in the tumor, expressed as a percentage of the injected dose, varied from 0.05% to 0.17%; the uptake per gram of tumor tissue varied from 0.0045% to 0.0124%.

DISCUSSION

Successful in vivo visualization of 29 of 31 paragangliomas in 20 patients using ^{123}I-Tyr^3-octreotide was previously reported (*7*). In addition, 13 of 14 paragangliomas investigated with in vitro autoradiography were shown to contain somatostatin receptors (*13*). The present study presents a detailed comparison of in vivo ^{111}In-octreotide scintigraphy with other imaging modalities used in the diagnosis and follow-up of patients referred for known paragangliomas or in whom a paraganglioma was suspected. Fifty of 53 (94%) known localizations in 25 patients with paragangliomas were visualized. In two patients, three localizations were missed during octreotide scintigraphy. This is probably due to the fact that the localizations were too small or contained an extremely low density of somatostatin receptors, or a combination of these, to be detected during octreotide scintigraphy.

In eight of nine patients in whom routine imaging failed to demonstrate paragangliomas, octreotide scintigraphy was also negative. In three patients, other pathology was demonstrated. This implies that octreotide scintigraphy can be used to help differentiate paraganglioma from other pathology, although it cannot, of course, differentiate paraganglioma from other somatostatin receptor positive tumors, i.e., other APUDomas.

High-resolution CT scanning in combination with MRI, with and without gadolinium-DTPA enhancement, is an effective imaging regime for paragangliomas and has limited the use of angiography to those cases where preoperative embolization is required (*14–17*). However, this type

TABLE 2
Uptake of ^{111}In-Octreotide in Tumors from Four Patients

Patient no.	Paraganglioma localization	T-to-B ratio	Tumor volume (cm^3)	%Uptake	%Uptake/g
4	Mediastinum	4.4	38.0	0.17	0.0045
16	Carotid body	2.1	8.7	0.06	0.0069
18	Carotid body	1.8	7.5	0.05	0.0063
22	Spine	2.4	9.2	0.11	0.0124

Calculations were performed on data obtained 24 hr after injection of ^{111}In-octreotide. T-to-B ratio = tumor-to-background radioactivity ratio; %Uptake = uptake of radioactivity as a percentage of the injected dose.

of imaging is usually limited to the site where a paraganglioma is clinically suspected. In our series, CT scanning or MRI of the site where a paraganglioma was primarily expected was in most cases combined with ultrasound of the neck, in order to detect multicentricity. With octreotide scintigraphy, however, unexpected additional paraganglioma sites not detected or not investigated with conventional imaging techniques were found in 9 of 25 patients (36%) with known paragangliomas. In four of them, the supposed tumor localizations also were demonstrated with other imaging modalities. This finding is of special interest since multicentricity and distant metastases may occur in 10% of patients (*1–3,18*). In this respect, one of the major advantages of octreotide scintigraphy is that it provides information on potential tumor sites in the whole body. It could thus be used as a screening test to be followed by CT scanning, MRI or ultrasound of the sites with abnormalities.

Surgery for carotid body and small jugulotympanic paragangliomas is usually successful, but surgical complications and mortality are high for larger tumors (*19*). Because of its high sensitivity in detecting paragangliomas, octreotide scintigraphy should be used as a screening modality in patients at risk, (i.e., in patients with known paraganglioma and in relatives of patients with familial paraganglioma) in order to detect paraganglioma sites at an early stage when surgery may be potentially less hazardous.

In patients who had surgery for paraganglioma, recurrence or residual tumor is observed in 10% of carotid body paragangliomas and in 29%–50% of jugulotympanic paragangliomas (*4,20*). Differentiation between recurrent or residual tumor and scar tissue may be difficult in these patients. In the present series, five of six recurrent or residual paragangliomas were visualized during octreotide scintigraphy. Therefore, octreotide scintigraphy could be useful in the follow-up of surgery patients, although studies in larger patient groups are required to evaluate octreotide scintigraphy in this respect.

In a recent study, visualization of paragangliomas using MIBG scintigraphy was reported in 8 of 15 patients (*21*). In our series, ^{123}I-MIBG uptake was found in only 2 of 5 patients with known paragangliomas, in whom tumors readily accumulated labeled octreotide. Therefore, octreotide scintigraphy is preferable to MIBG scanning for tumor imaging in paraganglioma patients.

Tumor-to-background ratios of radioactivity 24 hr after injection of ^{111}In-octreotide were calculated in four patients and varied from 1.8 to 4.4. This implies that clear visualization of paragangliomas with octreotide scintigraphy is possible. Radioactivity uptake is within the range reported for some monoclonal antibodies (*22,23*). Once a suitable somatostatin analogue to which a beta-emitting radionuclide can be coupled has been developed, studies can be conducted to determine sufficient uptakes for radiotherapy.

ACKNOWLEDGMENT

This work was supported by a grant from the Dutch National Health Service Board (Ziekenfondsraad).

REFERENCES

1. Capella C, Riva C, Cornaggia M, Chiaravalli AM, Frigerio B. Histopathology, cytology and cytochemistry of pheochromocytomas and paragangliomas including chemodectomas. *Path Res Pract* 1988;183:176–187.
2. Grufferman S, Gillman MW, Pasternak LR, Peterson CL, Young WG Jr. Familial carotid body tumors: case report and epidemiologic review. *Cancer* 1980;46:2116–2122.
3. Kliewer KE, Wen DR, Cancilla PA, Cochran AJ. Paragangliomas: assessment of prognosis by histologic, immunohistochemical, and ultrastructural techniques. *Hum Pathol* 1989;20:29–39.
4. Lack EE, Cubilla AL, Woodruff JM. Paragangliomas of the head and neck region. A pathologic study of tumors from 71 patients. *Hum Pathol* 1979; 10:191–218.
5. Krenning EP, Bakker WH, Breeman WAP, et al. Localisation of endocrine-related tumours with radioiodinated analogue of somatostatin. *Lancet* 1989; I:242–244.
6. Lamberts SWJ, Hofland LJ, van Koetsveld P, Reubi JC, Bakker WH, Krenning EP. Parallel in vivo and in vitro detection of functional somatostatin receptors in human endocrine pancreatic tumors: consequences with regard to diagnosis, localization, and therapy. *J Clin Endocrinol Metab* 1990;71:566–574.
7. Lamberts SWJ, Bakker WH, Reubi JC, Krenning EP. Somatostatin-receptor imaging in the localization of endocrine tumors. *N Engl J Med* 1990; 323:1246–1249.
8. Kwekkeboom DJ, Krenning EP, Bakker WH, et al. Radioiodinated somatostatin analog scintigraphy in small cell lung cancer. *J Nucl Med* 1991;32: 1845–1848.
9. Lamberts SWJ, Krenning EP, Reubi JC. The role of somatostatin and its analogs in the diagnosis and treatment of tumors. *Endocrinol Rev* 1991;12: 450–482.
10. Bakker WH, Krenning EP, Reubi JC, et al. In vivo application of [^{111}In-DTPA-D-Phe^1]-octreotide for detection of somatostatin receptor-positive tumors in rats. *Life Sci* 1991;49:1593–1601.
11. Krenning EP, Bakker WH, Kooij PPM, et al. Somatostatin receptor scintigraphy with [^{111}In-DTPA-D-Phe^1]-octreotide in man: metabolism, dosimetry and comparison with [^{123}I-Tyr^3]-octreotide. *J Nucl Med* 1992;33:652–658.
12. Bakker WH, Albert R, Bruns C, et al. [^{111}In-DTPA-D-Phe^1]-octreotide, a potential radiopharmaceutical for imaging of somatostatin receptor-positive tumors: synthesis, radiolabeling and in vitro validation. *Life Sci* 1991;49: 1583–1591.
13. Reubi JC, Waser B, Khosla S, et al. In vitro and in vivo detection of somatostatin receptors in pheochromocytomas and paragangliomas. *J Clin Endocrinol Metab* 1992;74:1082–1089.
14. Som PM, Sacher M, Stollman AL, Biller HF, Lawson W. Common tumors of the parapharyngeal space: refined imaging diagnosis. *Radiology* 1988;169: 81–85.
15. Jackson CG, Welling DB, Chironis P, Glasscock ME, Woods CI. Glomus tympanicum tumors: contemporary concepts in conservation surgery. *Laryngoscope* 1989;99:875–884.
16. Phelps PD. Glomus tumours of the ear: an imaging regime. *Clin Radiol* 1990;41:301–305.
17. Phelps PD, Cheesman AD. Imaging jugulotympanic glomus tumors. *Arch Otolaryngol Head Neck Surg* 1990;116:940–945.
18. Odze R, Bégin LR. Malignant paraganglioma of the posterior mediastinum. *Cancer* 1990;65:564–569.
19. Hodge KM, Byers RM, Peters LJ. Paragangliomas of the head and neck. *Arch Otolaryngol Head Neck Surg* 1988;114:872–877.
20. Farrior J. Surgical management of glomus tumors: endocrine-active tumors of the skull base. *South Med J* 1988;81:1121–1126.
21. Van Gils APG, van der Mey AGL, Hoogma RPLM, et al. Iodine-123-metaiodobenzylguanidine scintigraphy in patients with chemodectomas of the head and neck region. *J Nucl Med* 1990;31:1147–1155.
22. Divgi CR, Larson SM. Radiolabeled monoclonal antibodies in the diagnosis and treatment of malignant melanoma. *Semin Nucl Med* 1989;29:252–261.
23. Goldenberg DM, Goldenberg H, Sharkey RM, et al. Imaging of colorectal carcinoma with radiolabeled antibodies. *Semin Nucl Med* 1989;29:262–281.